Advances in Health Sciences Research, volume 40
2nd International Conference on Contemporary Science and Clinical Pharmacy 2021 (ICCSCP 2021)

Molecular Dynamics, Prediction of Toxicity, and Interaction of the Active Compound *Caesalpinia sappan* on Essential Lipids *Klebsiella pneumoniae*

Purnawan Pontana Putra[1]*, Fithriani Armin[1], Nola Florida[1], Gio Vanny Yusuf[1], Netty Suharti[1]

[1]*Faculty of Pharmacy, Universitas Andalas, Padang, 25163, Indonesia*
**Corresponding author. E-mail: purnawanpp@phar.unand.ac.id*

ABSTRACT
Pneumonia is the highest cause of death in the world. The presence of COVID-19 can worsen the patient's condition. One of the causes of pneumonia is *Klebsiella pneumoniae*. These bacteria can be resistant to antibiotics. In this case, an alternative treatment is needed. *Caesalpinia sappan*, based on pre-clinical trials, has an activity to be used as an antimicrobial. The activity predictions, molecular docking, and molecular dynamics simulations were performed using computational methods. The log P values were found in the range of 0.86-2.26. The molecular weights were in the range of 272.25-344.36 g/mol. All active compounds qualify with the Lipinski rule of 5. The lowest binding affinity value is -9.8 (kcal/mol), suggesting it can bind more strongly to the lipid from *Klebsiella pneumoniae*. Structure alert was obtained, namely catechol and aldehyde. The results of molecular dynamics of compound 7 in *Klebsiella pneumonia* protein got an eigenvalue of 5.186e-05. The active compound from *Caesalpinia sappan* is predicted to develop as a lipid inhibitor from *Klebsiella pneumoniae*. It has interaction such as Compound 7 has one hydrogen bond in the amino acid Trp46, one π-cation in Arg80, and one π-Sulfur bond in Met156.
Keywords: Pneumonia, *Klebsiella pneumoniae, Caesalpinia sappan, computational methods.*

1. INTRODUCTION

Pneumonia is the leading cause of death worldwide, especially in the age group, infants and children. This number of deaths globally exceeds the deaths of malaria, tuberculosis, and HIV infection combined. Pneumonia can be caused by bacteria, viruses, and mycoplasma [1]. *Klebsiella pneumoniae* bacteria are capable of infecting and exacerbating patients with COVID-19 disease [2].

These bacteria have become resistant to antibiotics [3]. Being a hospital-associated pathogen, Klebsiella is constantly exposed to many antibiotics that cause mutations [4]. The mechanism of polymyxin resistance in *Klebsiella pneumoniae* is a modification of the target by changing the lipopolysaccharide structure on the chromosome, thereby interfering with the binding of polymyxin to Lipid A (lpxM and its regulator ramA) [5].

The essential lipids in *Klebsiella pneumoniae* are enzymes that are stored in most gram-negative bacteria. It is a new antibiotic target. Where the target of the sulfonyl piperazine compound is LpxH [6]. Research on lipids is still new and becomes a challenge for future research.

Caesalpinia sappan has the potential as an antimicrobial [7]. Ethanol extract from this plant has the antibacterial potential [8]. Extracts from the bark of this plant can inhibit the growth of *Klebsiella pneumoniae* [9]. *Caesalpinia sappan* needs to be carried out molecular analysis with computational methods to predict how the potential of the active compound interacts with essential lipids from *Klebsiella pneumoniae*.

Previous studies combining computational and experimental research have shown that *Caesalpinia sappan* has activity against *Staphylococcus aureus* [10]. The molecular docking technique uses the mechanism of putative phytochemicals to reveal their interactions and biological therapeutic capabilities in the target active site,

with precise quality modeling of biomolecules, Molecular Dynamics (MD) simulation reveals the dynamic behavior of biomolecules at the atomic level [11]. Natural compound analyzed for their effects are single compounds because they are more specific to the target protein [12]. This study analyzed the chemical, physical properties, interactions between the active compounds and proteins, and molecular dynamics.

We discuss prediction with a computational approach. The use of computing in the field of research and development of new drugs can reduce the use of materials, reduce the use of experimental animals, and compare in vivo and in vitro tests.

Table 1. Analysis of Physicochemical Properties and Toxicity Prediction

Compound	Molecular Weight (g/mol)	Log P	Lipinski	Structure alert
1	344.36	2.26	Yes	Catechol
2	286.28	1.52	Yes	Catechol
3	272.25	1.64	Yes	Catechol
4	302.28	1.06	Yes	Catechol dan Aldehid
5	288.30	1.86	Yes	Catechol
6	316.31	0.86	Yes	Catechol
7	302.28	1.30	Yes	Catechol
8	286.28	2.17	Yes	Catechol

2. METHODS

2.1. Geometry Optimization and ADME Prediction

The active compound *Caesalpinia sappan* [13] which will be used in this study, is codenamed 1-8. The molecular structure of the test compound was first drawn using Marvin Sketch. Then the geometry was optimized using Avogadro software by selecting Force Field MMFF94. ADME prediction using a web-based application such as pkCSM and SWISS ADME [14] [15].

2.2. Preparation of Macromolecules and ligands

The target macromolecule used in the study was downloaded first on the website (www.rcsb.org). It is a receptor on *Klebsiella pneumoniae* (6pib) [6]. The crystal structure of the target macromolecule that was downloaded from the Protein Data Bank website was then prepared using MGLTools 1.5.6 software. This stage of preparation of target macromolecules is carried out by removing water molecules and natural ligands and adding hydrogen atoms and Kollman partial charges. Molecular Docking Using Autodock Vina software, by selecting 100 binding modes.

2.3. Identification of Docking and Molecular Dynamic Simulation Results

The results of the molecular docking simulation using autodock vina were selected from the minimum bond free energy, then analyzed for each residue involved, and analyzed the molecular interactions formed between macromolecules and the molecules of the test compound. Amino acid residues that play a role in the molecular interactions formed were analyzed for the type of bond using BIOVIA Discovery Studio 2020. Molecular dynamic studies were carried out to analyze Deformability, B-Factor, Eigenvalue, and Variance between ligands and proteins. The software used to analyze molecular dynamics is iMODS.

3. RESULTS AND DISCUSSION

Molecular weight analysis, log p, Lipinski, and structure alert were performed on the eight active compounds *Caesalpinia sappan*. The analysis results obtained eight (Table 1) compounds that met the Lipinski rule of five as well-absorbed drugs orally because they have molecular weight values <500 and Log P<5. The structural alert was acquired in the toxicity study, namely catechol and aldehyde in the active compound. Catechol groups have hepatotoxic characteristics and can create difficulties with aberrant liver function [16].

Catechol has a high iron affinity because it has two oxygen donor atoms and delocalized electrons through the conjugated ring [17]. Besides catechol, there is also an aldehyde group. The aldehyde group has the property of being easy to react with biomolecules and change their function. The aldehyde group is also capable of causing

Table 2. Predictive value of absorption metabolism distribution and excretion (ADME)

Compound	Absorption			Distribution		Metabolism			Excretion
	WS	Pgs	Skin-P	BBB-P	CNS-P	CYP1A2	CYP2C19	CYP3A4	TC
1	-3.847	Yes	-2.776	-1.05	-3.072	Yes	Yes	No	0.166
2	-3.346	Yes	-2.735	-0.748	-2.421	Yes	No	No	0.212
3	-3.239	Yes	-2.754	-0.873	-2.351	Yes	No	No	0.511
4	-3.571	Yes	-2.735	-0.94	-3.354	Yes	No	No	0.519
5	-3.334	Yes	-2.736	-0.841	-2.318	Yes	No	No	0.494
6	-2.749	Yes	-3.669	-0.827	-3.027	No	No	No	0.154
7	-3.141	Yes	-2.741	-0.937	-3.251	Yes	No	No	0.078
8	-3.019	Yes	-2.895	-0.981	-2.498	Yes	Yes	Yes	0.129

Information:

WS: Water Solubility (log mol/L)
Pgs: P-glycoprotein substrate
Skin-P: Skin Permeability (logKp)
BBB-P: blood-brain barrier Permeability (log BB)
CNS-P: Central Nervous System Permeability (log PS)
TC: Total Cleareance (log ml/min/kg)

oxidative stress and can turn into radicals [18]. This prediction is limited by looking at the toxic nature of the functional group of a compound. The toxicity test is much more accurate when using *in vivo*, *in vitro*, and clinical trials. These eight compounds have water solubility values in the range <-2 (Table 2), which are categorized as soluble in water [19]. All compounds can be absorbed on the P-glycoprotein substrate, which is a protein that functions as a pump to remove foreign objects from the cell. A compound has low skin permeability if log Kp > -2.5. All compounds were absorbed in the blood-brain barrier because they had a molecular weight of <400 and had hydrogen bonds <8. The lowest BBP-P value in compound 1 was influenced by the most significant molecular weight of 344.36 g/mol Compound 4 has the lowest CNS-P value, which is -3.354.

Drug distribution in the CNS-P depends on several factors such as cerebral blood flow, extracellular fluid, intracellular fluid, and pH [20]. From the predicted Metabolism, compound 6 is not metabolized to CYP1A2. CYP1A2 is abundant in the liver. Drugs metabolized to CYP1A2 include theophylline, caffeine, clozapine, olanzapine, tizanidine, duloxetine, and ramelteon [21].

Compounds 1 and 8 are metabolized at CYP2C19. CYP2C19 plays a role in the Metabolism of drugs, such as antiepileptic drugs (S-mephenytoin and diazepam), proton pump inhibitors (omeprazole), amitriptyline, citalopram, and propranolol [22]. Compound 8 is metabolized at CYP3A4. Metabolism of CYP3A4 is associated with the activity of HIV protease inhibitors, calcium channel blockers (nifedipine), hydroxymethylglutaryl inhibitors, coenzyme A reductase, antineoplastic drugs (cyclophosphamide, ifosfamide, docetaxel, paclitaxel, doxorubicin, etoposide, teniposide), or vinca alkaloids.

Metabolites include testosterone and aflatoxins [23]. Compound 7 is a compound that takes a long time to be

Table 3. Optimization of geometry and docking score.

Compound	Total Energy (kJ/mol)	Docking Score (kkal/mol)
1	451.076	-8.5
2	339.594	-8.1
3	361.128	-8.1
4	368.094	-7.3
5	432.081	-7.5
6	591.292	-7.3
7	317.349	-9.8
8	1977.63	-8.9

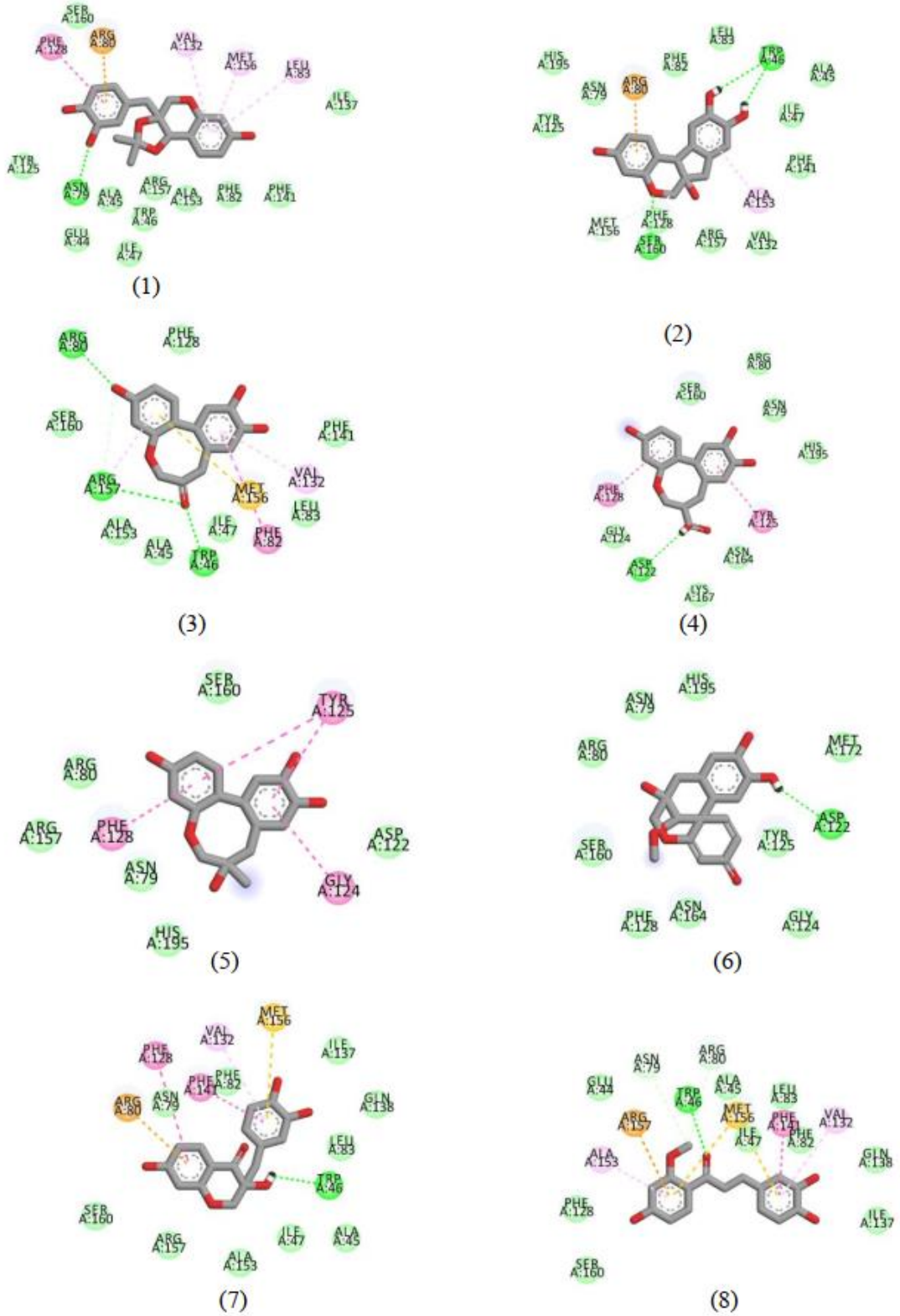

Figure 1. Predicted Interaction between active compounds from *Caesalpinia sappan* on Essential Lipids *Klebsiella pneumoniae*

eliminated in the body because it has the lowest Total Clearance value. Geometry optimization is carried out to

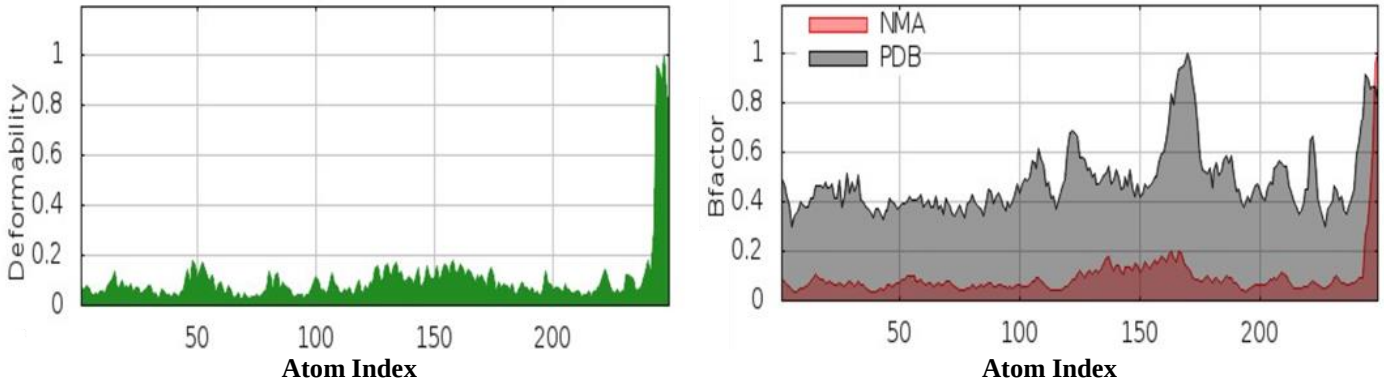

a) b)

Figure 2. a) Deformability relationship with atomic index b) B-Factor relationship with atom index.

calculate electronic structures quickly and efficiently[24].

Geometry optimization (Table 3) in the context of electronic structure calculations to search for minimum energy structures and transition structures [25]. The selected Force Field is MMFF94. The purpose of geometry optimization is to obtain a stable compound conformation with the lowest energy.

Molecular docking in this study using the Autodock Vina software. The validation of the docking method is carried out to ensure that the docking method has an accurate geometric pose. The Redocking technique is the docking of native ligands to proteins. The RMSD recommendation value is 2.0 [26].

The validation results obtained an RMSD value has 0.3. The lowest binding affinity value is -9.8 (kcal/mol), where it can be predicted bind more strongly to the lipid from *Klebsiella pneumoniae* (Table 3). We also predict the type of bond between the active compound and the protein (Figure 1). In compound 1, there is one hydrogen bond in Asn79, three π-alkyl interactions in Val132, Met156, and Leu83. Hydrogen bonding has a profound impact on protein folding and structure [27]. Compound 2 have Hydrogen bonds on Ser160 and Trp46, two van der Waals bonds in Met156 and Phe128, one π-Cation bond in Arg80, one π-Alkyl bond in Ala153. Compound 3 have hydrogen bonds in Trp46, Arg157, Arg80. One interaction π-π T-shaped bond in Phe82, two π-Alkyl bonds in Val132, and Arg157, one π-Sulfur bond in Met156. π-sulfur bonds can form a barrier that prevents dopamine from binding further to the intracellular surface[28].

Compound 4 has one hydrogen bond, two π-π bonds Stacked on Phe128 and Tyr125. Compound 5 has three π-π stacked interactions in Phe128, Tyr125 and Gly124.

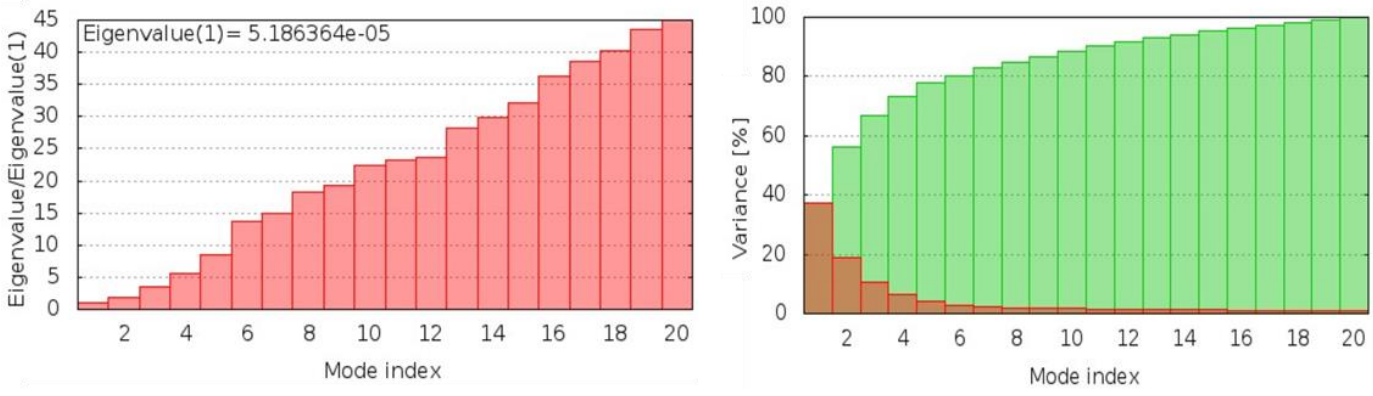

a) b)

Figure 3. a) Relationship of Eigen Value with Mode Index, b) Relationship between Variance and Mode Index.

Compound 6 has one hydrogen bond in Asp122. Compound 7 contains one hydrogen in Trp46, one bond π-cation in Arg80, one π-Sulfur bond in Met156. Compound 8 contains one hydrogen bond, one π-cation bond, one π-sulfur bond in Met156, one bond π-π stacked bond, and two bond π-alkyl bonds in Ala153 and Val132. Hydrogen-bonding can increase the receptor-ligand interaction when the donor and acceptor are significantly more potent, or the H-bond ability is weaker than the hydrogen and oxygen atoms in water [29].

π-cation bonds are significant for the function and pharmacology of ion channels and membrane proteins. These bonds are mostly found on aromatic rings (Phe, Tyr, or Trp) or interacting ligands [30].

The Variance is inversely related to the eigenvalues. Colored bars show individual (red) and cumulative (green) variances, and an increase in the cumulative Variance (Figure 3b) of the index mode but a decrease in individual variants.

The residual covariance matrix (Figure 4a) that undergoes correlated (red), uncorrelated (white), or anti-correlated (blue) motions. The correlation matrix is calculated using the coordinates and the Cα Cartesian equation. Each point in the graph represents one spring between the corresponding pairs of atoms. The darker gray color (Figure 4b) indicates a stiffer atomic motion.

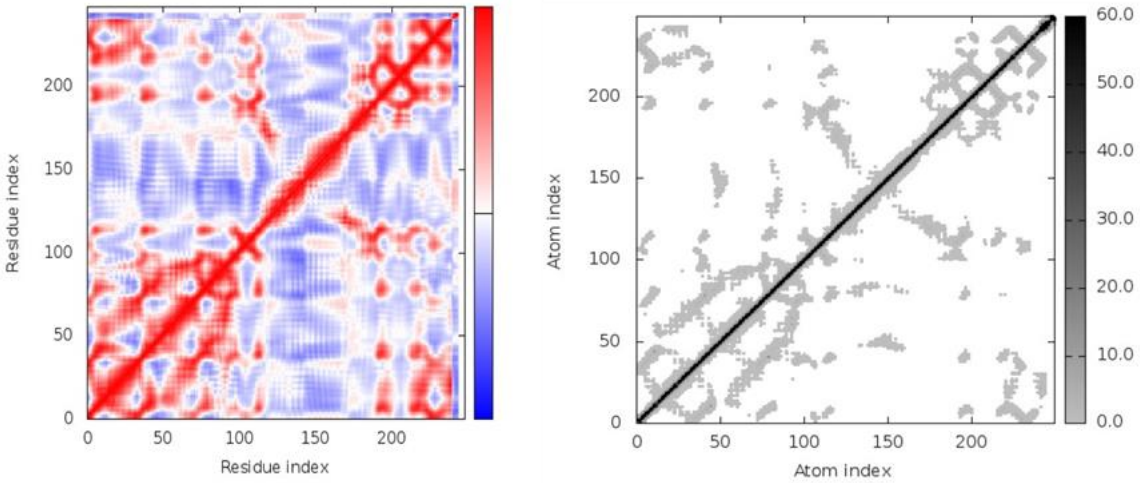

a) **b)**

Figure 4. Covariance and correlation matrix on a) Residue Index b) atomic index

Furthermore, compound 7 was analyzed by molecular dynamic simulation to see its deformability, B-Factor, Eigenvalue, Variance, and residue index. Deformability is a measure of the ability of a molecule to deform at each residue [31]. The index atom 240-250 tends to deform at the residue (Figure 2a). Normal Mode Analysis (NMA) is an approach to describe the collective functional movement of macromolecules. NMA consists of deformation vectors and frequencies, which describe atomic displacements and motion amplitudes [31].

The B-factor indicates the exact position of the atoms. The atomic positions always form irregularities in the crystal form. The higher the B-factor value, the higher the mobility and flexibility of a crystal [32]. The highest B-factor value (Figure 2b) is one at atomic index 160-170. The eigenvalue indicates the stiffness of motion of a protein. The eigenvalue is directly related to the energy required to change the shape of the protein structure. The lower the eigenvalue, the easier it is to change shape. The eigenvalue (Figure 3a) increases for each index mode.

4. CONCLUSION

The active compounds from *Caesalpinia sappan* can be candidates for drugs absorbed orally. The lowest free bond energy is obtained from the docking of compound 7. The type of bond that interacts is from ligands and proteins such as hydrogen bonds, π bonds, and Van der Waals bonds. Deformability, B-Factor, Eigenvalue, Variance, and residue index was analyzed molecular dynamics. The data shows index atom 240-250 tends to deform at the residue. The highest point on the B-Factor is at the atomic index of 160-170. Based on prediction, *Caesalpinia sappan* have the potential to be developed as a lipid inhibitor for *Klebsiella pneumoniae*.

AUTHORS' CONTRIBUTIONS

P.P.P contributed by performing the analysis, designed research, and wrote the paper. F.A, N.S

contributed by designed the study. N.F and G.V.Y contributed by collecting the data.

ACKNOWLEDGMENTS

Thanks to the Faculty of Pharmacy, Universitas Andalas for supporting this research with contract number 07/UN16.10.D/PJ.01./2021.

REFERENCES

[1] S. R. C. Howie, D. H. Hamer, and S. M. Graham, "Pneumonia," *Int. Encycl. Public Heal.*, pp. 500–508, 2016, doi: 10.1016/B978-0-12-803678-5.00334-9.

[2] G. Arcari *et al.*, "Klebsiella pneumoniae infections in COVID-19 patients: a 2-month retrospective analysis in an Italian hospital," *Int. J. Antimicrob. Agents*, vol. 57, no. 1, 2021, doi: 10.1016/j.ijantimicag.2020.106245.

[3] G. Montrucchio, S. Corcione, G. Sales, A. Curtoni, F. G. De Rosa, and L. Brazzi, "Carbapenem-resistant Klebsiella pneumoniae in ICU-admitted COVID-19 patients: Keep an eye on the ball," *J. Glob. Antimicrob. Resist.*, vol. 23, pp. 398–400, 2020, doi: 10.1016/j.jgar.2020.11.004.

[4] S. Navon-Venezia, K. Kondratyeva, and A. Carattoli, "Klebsiella pneumoniae: a major worldwide source and shuttle for antibiotic resistance," *FEMS Microbiol. Rev.*, vol. 013, pp. 252–275, 2017, doi: 10.1093/femsre/fux013.

[5] S. De Majumdar *et al.*, "Elucidation of the RamA Regulon in Klebsiella pneumoniae Reveals a Role in LPS Regulation," *PLoS Pathog.*, vol. 11, no. 1, pp. 1–22, 2015, doi: 10.1371/journal.ppat.1004627.

[6] J. Cho *et al.*, "Structural basis of the UDP-diacylglucosamine pyrophosphohydrolase LpxH inhibition by sulfonyl piperazine antibiotics," *Proc. Natl. Acad. Sci. U. S. A.*, vol. 117, no. 8, pp. 4109–4116, 2020, doi: 10.1073/pnas.1912876117.

[7] N. P. Nirmal and P. Panichayupakaranant, "Antioxidant, antibacterial, and anti-inflammatory activities of standardized brazilin-rich Caesalpinia sappan extract," *Pharm. Biol.*, vol. 53, no. 9, pp. 1339–1343, 2015, doi: 10.3109/13880209.2014.982295.

[8] R. Srinivasan *et al.*, "In vitro antimicrobial activity of Caesalpinia sappan L.," *Asian Pac. J. Trop. Biomed.*, vol. 2, no. 1 SUPPL., 2012, doi: 10.1016/S2221-1691(12)60144-0.

[9] A. N. Bukke, F. N. Hadi, and C. S. Produtur, "Comparative study of in vitro antibacterial activity of leaves, bark, heart wood and seed extracts of Caesalpinia sappan L.," *Asian Pacific J. Trop. Dis.*, vol. 5, no. 11, pp. 903–907, 2015, doi: 10.1016/S2222-1808(15)60954-9.

[10] C. F. Kuok *et al.*, "Synergistic antibacterial effects of herbal extracts and antibiotics on methicillin-resistant Staphylococcus aureus: A computational and experimental study," *Exp. Biol. Med.*, vol. 242, no. 7, pp. 731–743, 2017, doi: 10.1177/1535370216689828.

[11] H. Singh and N. Bharadvaja, "Treasuring the computational approach in medicinal plant research," *Prog. Biophys. Mol. Biol.*, vol. 164, pp. 19–32, 2021, doi: 10.1016/j.pbiomolbio.2021.05.004.

[12] P. P. Putra, A. Fauzana, and H. Lucida, "In Silico Analysis of Physical-Chemical Properties, Target Potential, and Toxicology of Pure Compounds from Natural Products," *Indones. J. Pharm. Sci. Technol.*, vol. 7, no. 3, p. 107, 2020, doi: 10.24198/ijpst.v7i3.26403.

[13] Y. Niu, S. Wang, C. Li, J. Wang, Z. Liu, and W. Kang, "Effective Compounds From Caesalpinia sappan L. on the Tyrosinase In Vitro and In Vivo," *Nat. Prod. Commun.*, vol. 15, no. 4, 2020, doi: 10.1177/1934578X20920055.

[14] D. E. V. Pires, T. L. Blundell, and D. B. Ascher, "pkCSM: Predicting small-molecule pharmacokinetic and toxicity properties using graph-based signatures," *J. Med. Chem.*, vol. 58, no. 9, pp. 4066–4072, 2015, doi: 10.1021/acs.jmedchem.5b00104.

[15] A. Daina, O. Michielin, and V. Zoete, "SwissADME: A free web tool to evaluate pharmacokinetics, drug-likeness and medicinal chemistry friendliness of small molecules," *Sci. Rep.*, vol. 7, no. March, pp. 1–13, 2017, doi: 10.1038/srep42717.

[16] C. Limban *et al.*, "The use of structural alerts to avoid the toxicity of pharmaceuticals," *Toxicol. Reports*, vol. 5, pp. 943–953, 2018, doi: 10.1016/j.toxrep.2018.08.017.

[17] H. K. Zane and A. Butler, "Fe Acquisition," *Compr. Inorg. Chem. II (Second Ed. From Elem. to Appl.*, vol. 3, pp. 1–20, 2013, doi: 10.1016/B978-0-08-097774-4.00301-6.

[18] R. M. Lopachin and T. Gavin, "Molecular mechanisms of aldehyde toxicity: A chemical perspective," *Chem. Res. Toxicol.*, vol. 27, no. 7, pp. 1081–1091, 2014, doi: 10.1021/tx5001046.

[19] A. Daina, O. Michielin, and V. Zoete, "SwissADME: A free web tool to evaluate pharmacokinetics, drug-likeness and medicinal chemistry friendliness of small molecules," *Sci. Rep.*, vol. 7, 2017, doi: 10.1038/srep42717.

[20] K. E. Warren, "Beyond the blood: Brain barrier: The importance of central nervous system (CNS) pharmacokinetics for the treatment of CNS tumors, including diffuse intrinsic pontine glioma," *Front. Oncol.*, vol. 8, no. JUL, 2018, doi: 10.3389/fonc.2018.00239.

[21] Z. Desta and D. A. Flockhart, "Pharmacogenetics of Drug Metabolism," *Clin. Transl. Sci. Princ. Hum. Res. Second Ed.*, pp. 327–345, 2017, doi: 10.1016/B978-0-12-802101-9.00018-1.

[22] R. P. B. K. W. Grody, Ed., *Emery and Rimoin's Principles and Practice of Medical Genetics and Genomics*, 7th Editio. Academic Press, 2018.

[23] Georg Hempel, "Drug Monitoring and Clinical Chemistry," Elsevier B.V, 2004.

[24] H. B. Schlegel, "Geometry optimization," *Wiley Interdiscip. Rev. Comput. Mol. Sci.*, vol. 1, no. 5, pp. 790–809, 2011, doi: 10.1002/wcms.34.

[25] J. Zheng and M. J. Frisch, "Efficient Geometry Minimization and Transition Structure Optimization Using Interpolated Potential Energy Surfaces and Iteratively Updated Hessians," *J. Chem. Theory Comput.*, vol. 13, no. 12, pp. 6424–6432, 2017, doi: 10.1021/acs.jctc.7b00719.

[26] J. C. Cole, C. W. Murray, J. W. M. Nissink, R. D. Taylor, and R. Taylor, "Comparing protein-ligand docking programs is difficult," *Proteins Struct. Funct. Genet.*, vol. 60, no. 3, pp. 325–332, 2005, doi: 10.1002/prot.20497.

[27] J. Gao, D. A. Bosco, E. T. Powers, and J. W. Kelly, "Localized thermodynamic coupling between hydrogen bonding and microenvironment polarity substantially stabilizes proteins," *Nat. Struct. Mol. Biol.*, vol. 16, no. 7, pp. 684–690, 2009, doi: 10.1038/nsmb.1610.

[28] K. N. M. Daeffler, H. A. Lester, and D. A. Dougherty, "Functionally important aromatic-aromatic and sulfur-π interactions in the D2 dopamine receptor," *J. Am. Chem. Soc.*, vol. 134, no. 36, pp. 14890–14896, 2012, doi: 10.1021/ja304560x.

[29] D. Chen, N. Oezguen, P. Urvil, C. Ferguson, S. M. Dann, and T. C. Savidge, "Regulation of protein-ligand binding affinity by hydrogen bond pairing," *Sci. Adv.*, vol. 2, no. 3, 2016, doi: 10.1126/sciadv.1501240.

[30] D. T. Infield, A. Rasouli, G. D. Galles, C. Chipot, E. Tajkhorshid, and C. A. Ahern, "Cation-π Interactions and their Functional Roles in Membrane Proteins: Cation-π interactions in membrane proteins," *J. Mol. Biol.*, vol. 433, no. 17, 2021, doi: 10.1016/j.jmb.2021.167035.

[31] J. R. López-Blanco, J. I. Aliaga, E. S. Quintana-Ortí, and P. Chacón, "IMODS: Internal coordinates normal mode analysis server," *Nucleic Acids Res.*, vol. 42, no. W1, 2014, doi: 10.1093/nar/gku339.

[32] Z. Sun, Q. Liu, G. Qu, Y. Feng, and M. T. Reetz, "Utility of B-Factors in Protein Science: Interpreting Rigidity, Flexibility, and Internal Motion and Engineering Thermostability," *Chem. Rev.*, 2019, doi: 10.1021/acs.chemrev.8b00290.